Exciton–phonon coupled states in CdTe / Cd 1x Zn x Te quantum dots

A. El Moussaouy, D. Bria, A. Nougauoi, R. Charrour, and M. Bouhassoune

Citation: Journal of Applied Physics **93**, 2906 (2003); doi: 10.1063/1.1540740
View online: http://dx.doi.org/10.1063/1.1540740
View Table of Contents: http://scitation.aip.org/content/aip/journal/jap/93/5?ver=pdfcov
Published by the AIP Publishing

Exciton–phonon coupled states in CdTe/$Cd_{1-x}Zn_xTe$ quantum dots

A. El Moussaouy, D. Bria,[a] and A. Nougauoi
Laboratoire de Dynamique et d'Optique des Matériaux, Département de Physique, Faculté des Sciences, Université Mohamed I, B.P. 524, 60000 Oujda, Morocco

R. Charrour
Theoretische Fysica van de Vaste Stoffen, Departement Natuurkunde, Universiteit Antwerpen (U.I.A.), Universiteitsplein 1, B-2610 Antwerpen, Belgium

M. Bouhassoune
Max-Planck-Institute für Mikrostrukturphysik, Weinberg 2, D-06120 Halle, Germany

(Received 18 September 2002; accepted 4 December 2002)

This article presents a theoretical analysis of the dependence of the exciton binding energy and exciton–LO-phonon coupling on the cylindrical quantum dot (QD) size. The effect of the temperature on the integrated photoluminescence line intensity is also investigated. Calculations were performed within the effective-mass approximation by using a variational method. Specific applications of these results are given for CdTe QDs embedded in a $Cd_{1-x}Zn_xTe$ matrix. The excitonic confinement is described by a finite, deep potential well. We observe, on the one hand, an enhancement of the exciton binding energy and the exciton–LO-phonon coupling energy with decreasing dot size. On the other hand, at high temperature, the LO phonon has a noticeable effect on the photoluminescence intensity. This last physical parameter also shows a great dependence on QD size and on the potential level induced by the barrier material. © *2003 American Institute of Physics.* [DOI: 10.1063/1.1540740]

I. INTRODUCTION

In recent years, a great deal of interest has been devoted to the study and the engineering of high-quality devices of very low dimensions, essentially quantum-well wires or quantum-dot (QD) semiconductors.[1–14] They are theoretically predicted to offer superior optical and electrical properties. Excitons play a dominant role in their physical properties, therefore, their stability is important for possible devices requiring this characteristic. The reduced dimensionality of these structures enhances the electron–hole overlap (excitonic effect). Thus, the binding energy increases when going from bulk to quantum wells, and then to quantum-well wires and QDs. The polaronic process has become a main research subject in the physics of low-dimensional systems.[15–18] This is due to the key role played by the optical phonons on the scattering of charge carriers, which is essential for the understanding of the experimental observation of the semiconductor optical spectra.[15,19] More recently, many papers have been devoted to this process and to its influence on various physical properties of polar semiconductor quantum wells and QDs.[16–27] Some recent optical measurements[20–22,28–32] of the photoluminescence (PL) spectra realized on different QDs and quantum-well semiconductor structures, also reveal the LO phonons' effect on the PL linewidths.

The purpose of this work is to study more specifically the effect of LO phonons on the binding energy of an exciton in a cylindrical QD of CdTe (well material), of radius R and height H, embedded in $Cd_{1-x}Zn_xTe$ (barrier material). The quantum confinement induced by the barrier material is described by a finite, deep potential well. The calculation of the exciton binding energy is performed within the framework of a variational approach in the effective-mass approximation (see Ref. 33). This calculation leads us to evaluate the effect of such a type of interaction on the integrated PL intensity, which represents one of the important parameters characterizing the optical properties of semiconductor structures. This effect will be depicted versus the temperature variation and for different values of the QD sizes and the potential level induced by $Cd_{1-x}Zn_xTe$ barrier material. As proposed by Kayanuma,[34] by varying the radius R and height H of the QD, we obtain the various limiting situations of the bulk, the quantum well, the quantum wire, and the quantum dot. Here, we are also interested in the dimensionality crossover in the critical confinement limit, for which the quantum confinement effect is rapidly overwhelmed by the bulk effect. After a brief introduction of the system Hamiltonian and the method of calculation in Sec. II, we present, in Sec. III, some numerical illustrations for the CdTe/$Cd_{1-x}Zn_xTe$ systems.

II. FORMALISM

The exciton Hamiltonian in a cylindrical QD of radius R and height $H=2d$ (well material) embedded in barrier material semiconductors, interacting with the optical phonons (confined LO), can be written within the framework of the effective-mass and nondegenerate-band approximations, as follows:

$$H = H_{\text{ex}} + H_{\text{LO}} + H_{\text{ex-LO}}, \tag{1}$$

where H_{ex} is the excitonic Hamiltonian given by

[a]Electronic mail: bria@sciences.univ-oujda.ac.ma

$$H_{\mathrm{ex}}=-\frac{\eta}{2m_{\mathrm{e}}^{*}}\nabla_{\mathrm{e}}^{2}-\frac{\eta^{2}}{2m_{\mathrm{h}}^{*}}\nabla_{\mathrm{h}}^{2}-\frac{e^{2}}{\varepsilon_{\infty}|r_{\mathrm{e}}-r_{\mathrm{h}}|}+V_{w}^{\mathrm{e}}(r_{\mathrm{e}})+V_{\mathrm{w}}^{\mathrm{h}}(r_{\mathrm{h}}),\tag{2}$$

where m_e^* and m_h^* are the effective masses of the electron and hole, respectively, and $r_{\mathrm{e}}=(\rho_{\mathrm{e}},z_{\mathrm{e}})$ and $r_{\mathrm{h}}=(\rho_{\mathrm{h}},z_{\mathrm{h}})$ are the spatial coordinates of the electron and hole, respectively. V_w^e (r_{e}) and V_w^h (r_{h}) are the corresponding confining potentials for the electron and hole, respectively:

$$V_{\mathrm{w}}^{i}(r_{i})=\begin{cases}0 & \text{if } \rho_{i}\leqslant R \text{ and } |z_{i}|\leqslant d\\ V_{i} & \text{elsewhere}\end{cases},\qquad (i=\mathrm{e,h}).\tag{3}$$

In the presence of the phonon modes, the Coulomb potential will be taken as $(\varepsilon_0/\varepsilon_\infty)2/\sqrt{\rho_{\mathrm{eh}}^2+(z_{\mathrm{e}}-z_{\mathrm{h}})^2}$, where ε_0 and ε_∞ are the low and high frequency dielectric constants, respectively.

In Eq. (1), H_{LO} and $H_{\mathrm{ex\text{-}LO}}$ are, respectively, the Hamiltonian operator for confined LO phonon and the exciton–LO-phonon interaction.

$$H_{\mathrm{LO}}=\sum_{l,n_1}\hbar\omega_{\mathrm{LO}}a_{l,n_1}^{+}a_{l,n_1},\tag{4}$$

where a_{l,n_1}^{+} (a_{l,n_1}) are creation (annihilation) operators for the LO phonon of the (l,n_1)th mode, with frequency ω_{LO} and wave vector $(k_{\parallel}=\chi_{n_1}/R, k_z=l\pi/2d)$ where χ_{n_1} is the n_1th root of the Bessel function of the zero order.

$$H_{\mathrm{ex\text{-}LO}}=H_{\mathrm{e\text{-}LO}}+H_{\mathrm{h\text{-}LO}},\tag{5}$$

$$H_{i\text{-}\mathrm{LO}}=-\sum_{n_1}J_0\left(\frac{\chi_{n_1}}{R}\rho_i\right)\times\left[\sum_{l=1,3\ldots}V_{l,n_1}\cos\left(\frac{l\pi_i}{2d}z_i\right)(a_{l,n_1}+a_{l,n_1}^{+})+\sum_{l=2,4\ldots}V_{l,n_1}\sin\left(\frac{l\pi_i}{2d}z_i\right)(a_{l,n_1}+a_{l,n_1}^{+})\right],\quad (i=\mathrm{e,h}),\tag{6}$$

where

$$V_{l,n_1}^{2}=\frac{1}{V}\frac{4\pi e^{2}\hbar\omega_{\mathrm{LO}}}{\left(\frac{\chi_{n_1}}{R}\right)^{2}J_1^{2}(\chi_{n_1})\left[1+\left(\frac{l\pi R}{2dx_{n_1}}\right)^{2}\right]}\left(\frac{1}{\varepsilon_\infty}-\frac{1}{\varepsilon_0}\right),\tag{7}$$

with $V=2\pi R^2 d$ is the volume of cylindrical dot.

To deal with the Hamiltonian of this system, we shall adopt the variational treatment for quasi-zero-dimensional systems developed in Ref. 35. The effective Hamiltonian, in the atomic units system ($a_{\mathrm{ex}}^{*}=\varepsilon_0\hbar^2/\mu e^2$ excitonic Bohr radius and Rydberg energy $R_{\mathrm{ex}}^{*}=\mu e^4/2\varepsilon_0^2\hbar^2$), reads

$$H_{\mathrm{eff}}=-\frac{1}{1+\sigma}\left[\frac{\partial^2}{\partial\rho_{\mathrm{e}}^2}+\frac{1}{\rho_{\mathrm{e}}}\frac{\partial}{\partial\rho_{\mathrm{e}}}+\frac{\rho_{\mathrm{eh}}^2+\rho_{\mathrm{e}}^2-\rho_{\mathrm{h}}^2}{\rho_{\mathrm{e}}\rho_{\mathrm{eh}}}\frac{\partial^2}{\partial\rho_{\mathrm{e}}\partial\rho_{\mathrm{eh}}}+\frac{\partial^2}{\partial z_{\mathrm{e}}^2}\right]-\frac{\sigma}{1+\sigma}\left[\frac{\partial^2}{\partial\rho_{\mathrm{h}}^2}+\frac{1}{\rho_{\mathrm{h}}}\frac{\partial}{\partial\rho_{\mathrm{h}}}+\frac{\rho_{\mathrm{eh}}^2+\rho_{\mathrm{h}}^2-\rho_{\mathrm{e}}^2}{\rho_{\mathrm{h}}\rho_{\mathrm{eh}}}\frac{\partial^2}{\partial\rho_{\mathrm{h}}\partial\rho_{\mathrm{eh}}}+\frac{\partial^2}{\partial z_{\mathrm{h}}^2}\right]$$
$$-\left[\frac{\partial^2}{\partial\rho_{\mathrm{eh}}^2}+\frac{1}{\rho_{\mathrm{eh}}}\frac{\partial}{\partial\rho_{\mathrm{eh}}}\right]-\frac{\varepsilon_0}{\varepsilon_\infty}\frac{2}{\sqrt{\rho_{\mathrm{eh}}^2+(z_{\mathrm{e}}-z_{\mathrm{h}})^2}}+V_{\mathrm{w}}^{\mathrm{e}}(\rho_{\mathrm{e}},z_{\mathrm{e}})+V_{\mathrm{w}}^{\mathrm{h}}(\rho_{\mathrm{h}},z_{\mathrm{h}})+V_{\mathrm{e\text{-}LO}}(\rho_{\mathrm{e}},z_{\mathrm{e}})+V_{\mathrm{h\text{-}LO}}(\rho_{\mathrm{h}},z_{\mathrm{h}})$$
$$+V_{\mathrm{e\text{-}LO\text{-}h}}^{\mathrm{ex}}(\rho_{\mathrm{e}},z_{\mathrm{e}},\rho_{\mathrm{h}},z_{\mathrm{h}}),\tag{8}$$

where $\sigma=m_{\mathrm{e}}^{*}/m_h^{*}$ and $V_{\mathrm{e\text{-}LO}}$ $(\rho_{\mathrm{e}},z_{\mathrm{e}})$ $[V_{\mathrm{h\text{-}LO}}(\rho_{\mathrm{h}},z_{\mathrm{h}})]$, $V_{\mathrm{e\text{-}LO\text{-}h}}^{\mathrm{ex}}$ $(\rho_{\mathrm{e}},z_{\mathrm{e}},\rho_{\mathrm{h}},z_{\mathrm{h}})$ are, respectively, the effective potentials induced by the electron (hole)–LO-phonon coupling and the electron–hole exchange potential via an LO phonon, these expressions are determined by using unitary transformation at low temperature limit:[27,36]

$$V_{i\text{-}\mathrm{LO}}(\rho_i,z_i)=-\sum_{n_1}\frac{J_0^{2}\left(\frac{\chi_{n_1}}{R}\rho_i\right)}{\hbar\omega_{\mathrm{LO}}}\left[\sum_{l=1,3\ldots}V_{l,n_1}^{2}\cos^{2}\left(\frac{l\pi_i}{2d}z_i\right)+\sum_{1=2,4\ldots}V_{l,n_1}^{2}\sin^{2}\left(\frac{l\pi_i}{2d}z_i\right)\right],\quad (i=\mathrm{e,h})\tag{9}$$

and

$$V_{\mathrm{e\text{-}LO\text{-}h}}^{\mathrm{ex}}(\rho_{\mathrm{e}},z_{\mathrm{e}},\rho_{\mathrm{h}},z_{\mathrm{h}})=\sum_{n_1}\frac{2J_0\left(\frac{\chi_{n_1}}{R}\rho_{\mathrm{e}}\right)J_0\left(\frac{\chi_{n_1}}{R}\rho_{\mathrm{h}}\right)}{\hbar\omega_{\mathrm{LO}}}\left[\sum_{l=1,3\ldots}V_{l,n_1}^{2}\cos\left(\frac{l\pi_{\mathrm{e}}}{2d}z_{\mathrm{e}}\right)\cos\left(\frac{l\pi_{\mathrm{h}}}{2d}z_{\mathrm{h}}\right)+\sum_{l=2,4\ldots}V_{l,n_1}^{2}\sin\left(\frac{l\pi_{\mathrm{e}}}{2d}z_{\mathrm{e}}\right)\sin\left(\frac{l\pi_{\mathrm{h}}}{2d}z_{\mathrm{h}}\right)\right].\tag{10}$$

In order to calculate the exciton binding energy, we choose the following wave function:[37]

$$\psi_{ex}=F_e(\rho_e,z_e)F_h(\rho_h,z_h)F_{eh}(\rho_{eh},|z_e-z_h|), \tag{11}$$

with

$$F_{eh}(\rho_{eh},|z_e-z_h|)=\exp(-\alpha\rho_{eh})\exp[-\gamma(z_e-z_h)^2], \tag{12}$$

$$F_i(\rho_i,z_i)=f_i(\rho_i)g_i(z_i), \quad (i=\text{e,h}), \tag{13}$$

respectively, the corresponding two-dimensional (lateral direction) and one-dimensional (longitudinal direction) effective-mass Schrödinger equations are

$$\left\{-\frac{\hbar^2}{2m_i^*}\nabla_i^2+V_w^i(\rho_i)\right\}f_i(\rho_i)=E_i f_i(\rho_i), \quad (i=\text{e,h}), \tag{14}$$

$$\left\{-\frac{\hbar^2}{2m_i^*}\nabla_i^2+V_w^i(z_i)\right\}g_i(z_i)=E_i g_i(z_i), \quad (i=\text{e,h}), \tag{15}$$

with solutions of the form

$$f_i(\rho_i)=\begin{cases} J_0\left(\theta_i\dfrac{\rho_i}{R}\right) & \text{for } \rho_i<R \\ A_iK_0(\beta_i\rho_i) & \text{for } \rho_i>R \end{cases} \quad (i=\text{e,h}), \tag{16}$$

$$g_i(z_i)=\begin{cases} \cos\left(\pi_i\dfrac{z_i}{2d}\right) & \text{for } |z_i|<d \\ B_i\exp(k_i|z_i|) & \text{for } |z_i|>d \end{cases} \quad (i=\text{e,h}). \tag{17}$$

J_m and K_m are the modified Bessel functions of mth order. θ_i, β_i, π_i, k_i, A_i, and B_i are determined from the boundary conditions.

In Eq. (12), α and γ are the variational parameters. The bound-state energy of the exciton–phonon interaction system can be written as

$$E=\min_{\alpha,\gamma}\langle\psi_{ex}|H_{eff}|\psi_{ex}\rangle. \tag{18}$$

The exciton–phonon binding energy is defined as the difference between the bound state energy of the exciton and the polaron self-energies of a free electron-polaron and a free hole-polaron.

The polaronic correction to the exciton binding energy is defined as the difference between the exciton binding energy in the presence and absence of the LO-phonon modes:

$$\Delta E_B=E_B^{ph}-E_B^S. \tag{19}$$

In relation to the optical experience on these QD structures, integrated PL intensity is one of the physical parameters able to draw a good picture of their optical properties. The temperature dependence of integrated PL intensity gives by the Arrhenius model:[28,38]

$$\frac{I(T)}{I(0)}=\frac{1}{1+C_1\exp\left(-\dfrac{E_1}{kT}\right)+C_2\exp\left(-\dfrac{E_2}{kT}\right)}, \tag{20}$$

where $I(T)$ and $I(0)$ are the integrated PL intensities emission at temperatures T and 0 °K, respectively, E_1 and E_2 are activation energies, and C_1 and C_2 are constants characterizing the ratio of nonradiative to radiative recombination rates.

$$E_1=E_e+E_h-\min_{\alpha,\gamma}\frac{\langle\psi_{ex}|H_{eff}|\psi_{ex}\rangle}{\langle\psi_{ex}|\psi_{ex}\rangle}, \tag{21}$$

$$E_2=E_e+E_h+E_{e\text{-LO}}+E_{h\text{-LO}}, \tag{22}$$

where E_e and E_h are, respectively, the electron and hole binding energies, and $E_{e\text{-LO}}$ and $E_{h\text{-LO}}$ are the coupling energies between electron and hole with LO phonons, respectively.

III. NUMERICAL RESULTS

In order to investigate the effect of the QD sizes on the exciton binding energy, we consider the case of a cylindrical QD made of CdTe embedded in $Cd_{1-x}Zn_xTe$ material. The physical parameters corresponding to the (well) polar crystal CdTe are: $\varepsilon_0=9.6$, $\varepsilon_\infty=7.13$, $m_{lh}^*=0.11m_0$, $m_{hh}^*=0.662m_0$, $m_e^*=0.098m_0$, [m_e^*, m_{lh}^*, and m_{hh}^* are respectively, the electron, the light-hole (lh) and heavy-hole (hh) effective mass] $\hbar\omega_{LO}=20.84$ meV and the electron–phonon coupling $\alpha_F=0.315$. Our numerical results are presented in units of the effective Rydberg energy $R_{ex}^*=7.62$ meV and of the effective Bohr radius $a_{ex}^*=98.17$ Å. Figures 1(a) [1(b)] show the variation of the binding energy of a lh exciton in a QD, as a function of the cylinder radius R for several fixed dot heights $H=1a_{ex}^*$, $2a_{ex}^*$, and $3a_{ex}^*$ (as a function of the cylinder height H for several fixed dot radius $R=1a_{ex}^*$, $2a_{ex}^*$ and $3a_{ex}^*$) and for a Zn concentration $x=0.30$, which correspond to given values of the electron and hole potential barrier heights of, $V_e=146.4$ meV and $V_h=42$ meV, respectively. The binding energy increases as the radius decreases (well width is reduced), reaches a maximum, and then decreases. This behavior is due to the finite confinement potential model considered here. At small R values, discrete exciton levels are absent in the well, and the electron and hole wave functions are distributed outside the cylinder. When increasing the cylinder radius R, the exciton energy levels fall from the continuum spectrum into the well. The exciton binding energy presents the same behavior versus the dot height H; it decreases with increasing dot height. This result is similar to that obtained by us in the case of a hydrogenic impurity in QDs.[36] Let us notice that it has been pointed out by Le Goff and Stebe[37] that the peak position of the binding energy as function of the radius R does not depend strongly on the value of the height H, which is still consistent with our results.

To emphasize the effect of both the barrier potential and the polaronic correction on the exciton binding energy, we illustrate, in Fig. 2, the binding energy without (dashed lines) and with LO phonons (solid lines) for different barrier potential values. Figures 2(a) and 2(b) give, respectively, the binding energy of the lh and hh exciton versus the dot radius for dot height $H=1a_{ex}^*$, and for three values of the Zn concentration: $x=0.08$ ($V_e=34.1$ meV, $V_h=12$ meV), $x=0.16$ ($V_e=71.4$ meV, $V_h=24.1$ meV), and $x=0.3$ ($V_e=146.4$ meV, $V_h=42$ meV). From this figure, we understand

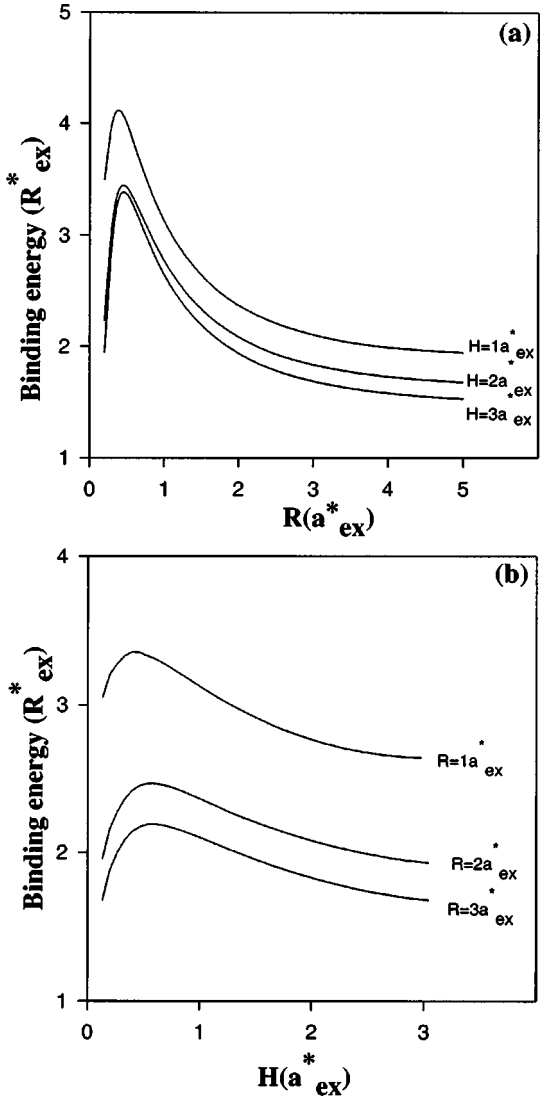

FIG. 1. Binding energy of an exciton confined in a CdTe QD as a function of: (a) the cylinder radius R for three values of the height ($H=2d$) and (b) the cylinder height ($H=2d$) for three values of the radius R.

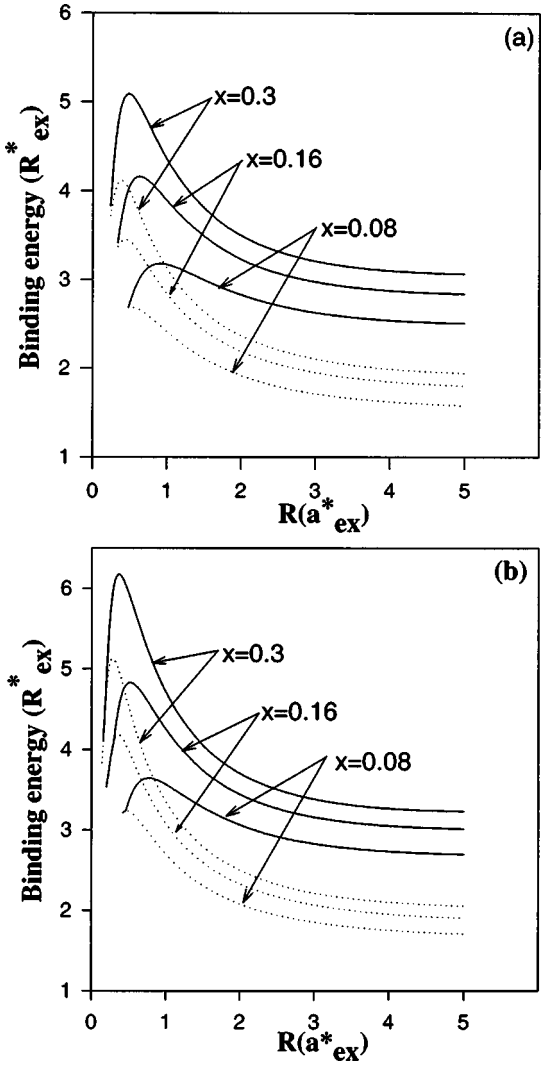

FIG. 2. Variation of (a) lh and (b) hh exciton binding energies as function of the cylinder radius R for three values of Zn concentration x (three values of barrier potential height). The solid and dotted curves represent the binding energies with and without the phonon correction, respectively.

that the variations of the exciton binding energy with the Zn concentration x (well depth) are very important. Besides, the shape of the curves obtained with and without LO phonon modes are similar. The correction due to the phonon modes is more pronounced as the exciton binding energy becomes larger. Furthermore, including the phonon mode effect, the exciton state will be the most stable if the dot radius is in the range of 0.3 to $0.6a^*_{ex}$ (strong confinement regime).

In Fig. 3 we give, with dashed and solid lines, respectively, the polaronic correction to the binding energy of lh and hh exciton in CdTe QD of height $H=1a^*_{ex}$, embedded in a $Cd_{1-x}Zn_xTe$ barrier material of Zn concentration $x=0.30$, as a function of the QD radius R. The confined LO-phonon effect is more important for hh excitons, and it is more pronounced in the region of the strong confinement regime.

Including the effect of the LO phonons, we have presented, in Figs. 4(a) and 4(b), the variation of the hh and lh exciton binding energy, respectively, as a function of both the height H and the radius R of the cylindrical QD. For each type of exciton, the corresponding binding energy increases as the sizes of the dot are reduced, reaches a maximum, and then decreases. When the dot becomes smaller, the exciton wave functions are compressed, and the probability to find the electron and the hole outside increases. This representation clearly illustrates the transition between the various confinement geometries representative of the quasi-three-dimensional, quasi-two-dimensional, quasi-one-dimensional, and quasi-zero-dimensional (0D) cases. The present results support the belief that the excitonic states should be enhanced and more stable in the QD than in the wire and well.

One of the most recent interests in the area of QD physics has been to investigate the role of carrier charge (electron or hole) interaction not only on the electronic properties, but also on the optical ones. The investigation of emission spectra of such structures at different temperatures leads to an understanding of the exciton–phonon coupling, and to highlight the presence of the lateral migration.[20] Equation (20), giving the analytical expression of the integrated PL intensity, shows the dependence of this coefficient not only upon the temperature fluctuation, but also upon the activation en-

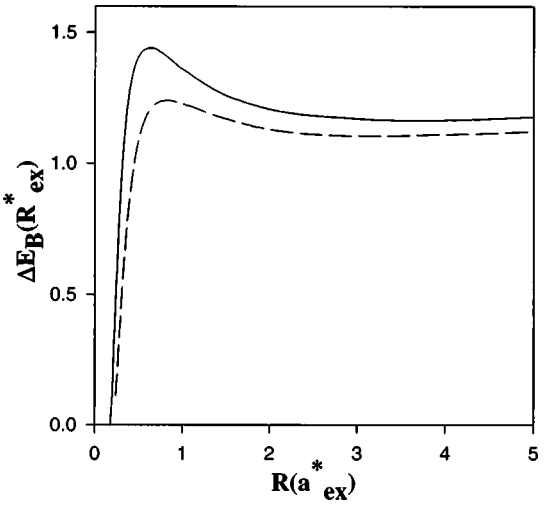

FIG. 3. Polaronic correction (ΔE_B) to the lh and hh exciton binding energies in the CdTe/$Cd_{1-x}Zn_xTe$ case as a function of the QD radius for a Zn concentration $x=0.3$ and $H=1a^*_{ex}$.

ergies E_1 [Eq. (21)] and E_2 [Eq. (22)], and the constants C_1 and C_2, characterizing the ratio of nonradiative to radiative recombination rates. Let us recall that the interaction of the exciton with optical phonons affects only the activation energies E_1 and E_2 [see Eqs. (21) and (22)], and thus the PL coefficient. Hence, it is convenient to know the effect of this type of interaction on the integrated PL intensity curve in terms of temperature. In order to achieve this aim and for the sake of simplicity to obtain the basic information about this process, we take the constant C_1 and C_2 equal unit.

Figure 5 displays the behavior of the integrated photoluminescence intensity versus the temperature inverse variation, with and without LO-phonon modes, of hh excitons in CdTe QDs embedded in a $Cd_{1-x}Zn_xTe$ barrier material in which the Zn fraction $x=0.3$. In Figs. 5(a) and 5(b), respectively, the integrated PL intensity is depicted for CdTe QDs of height $H=1a^*_{ex}$ and values of radius $R=1a^*_{ex}$, $1.5a^*_{ex}$, and $3a^*_{ex}$, and CdTe QDs of radius $R=1a^*_{ex}$ and of height $H=1a^*_{ex}$, $1.5a^*_{ex}$, and $3a^*_{ex}$. A first analysis of these curves leads to the conclusion that at high temperature, and for hh excitons, the LO phonons have a noticeable effect on the PL intensity. Moreover, it is convenient to note that the sizes of the QD have a great influence on the PL spectra versus the temperature variation. We observe that at high temperature, the intensity ratio $I(T)/I(0)$ decreases when increasing the radius R [Fig. 5(a)] or the height H [Fig. 5(b)]. We notice also that the intensity decreases more rapidly in the case of decreasing radius than decreasing height.

In Fig. 6 we show, for a given CdTe quantum dot of sizes $R=H=1a^*_{ex}$, how the depth of the barrier potential induced by the $Cd_{1-x}Zn_xTe$ material modifies the intensity of the integrated PL intensity ratio $I(T)/I(0)$. This is depicted for three values of the Zn fraction, corresponding to different values of the potential barriers levels, when taking into account the effect of the interaction of exciton with LO-phonon modes. We remark that at low temperature, the height of the potential barriers has no effect on the PL intensity ratio $I(T)/I(0)$, and, on the contrary, when the temperature increases and beyond a certain critical value of the temperature (around 40 °K), the well potential barrier noticeably influences PL spectra.

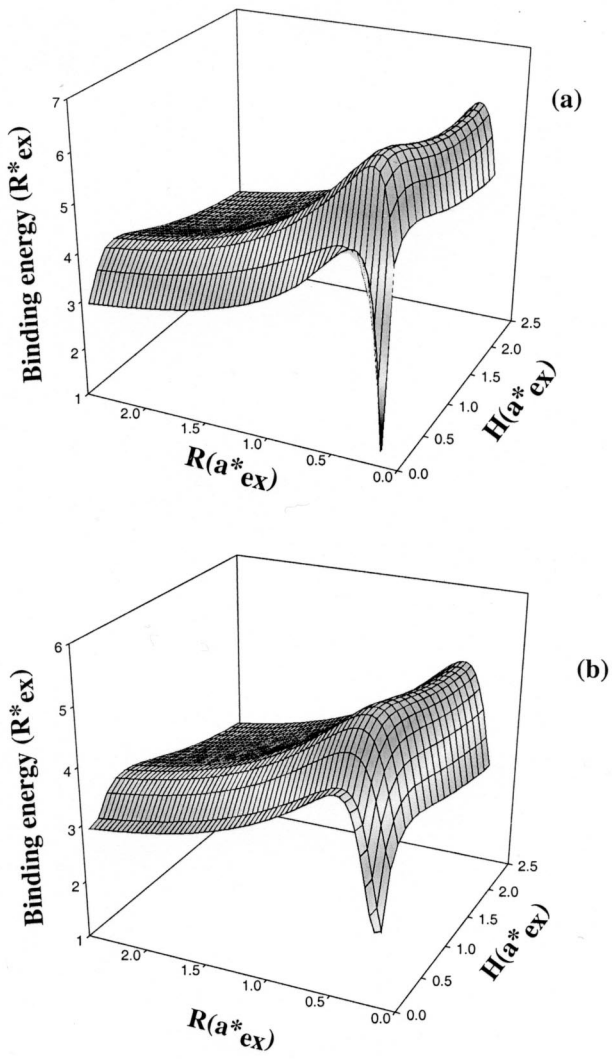

FIG. 4. Variation of the (a) hh and (b) lh exciton binding energies as a function of the radius R and the height H of the cylinder with the phonon correction for a Zn concentration $x=0.3$.

IV. CONCLUSION

By using the variational method to solve the effective-mass equation, we have investigated two effects on the excitonic binding energy for lh and hh with finite potential depth: the polaronic correction and the dot-size effect. Our results show that, due to the finite confining capacity of the QD, there is a critical radius for which the exciton is no longer confined. Indeed, as the confining potential decreases, this critical radius becomes bigger. We have also shown that the LO-phonon mode correction increases when the confinement sizes decrease. Furthermore, this correction is more important for the hh exciton. Calculation of the integrated PL intensity versus the temperature variation, and including the effect of the barrier of potential, shows the noticeable effect

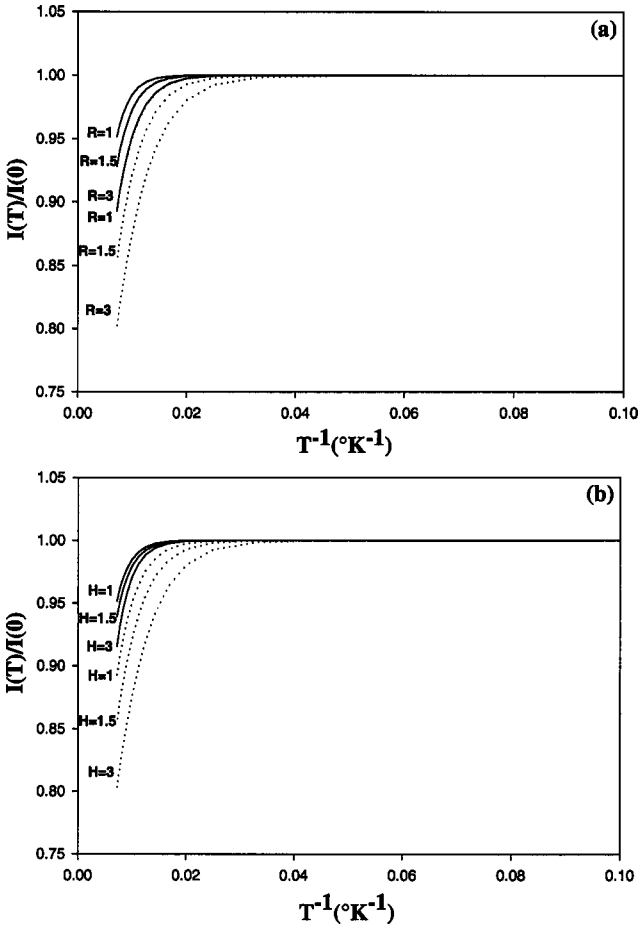

FIG. 5. Arrhenius plot of the integrated PL intensity using Eq. (22) in the case of $CdTe/Cd_{1-x}Zn_xTe$ as function of T^{-1} for a Zn concentration $x=0.3$. The solid lines are with phonons while the dotted lines are without phonons. (a) $H=1a_{ex}^*$, for three values of the dot radius $R=1a_{ex}^*$, $1.5a_{ex}^*$, $3a_{ex}^*$ and (b) $R=1a_{ex}^*$, for three values of the dot height $H=1a_{ex}^*$, $1.5a_{ex}^*$, $3a_{ex}^*$.

of the LO-phonon mode on the PL spectra. These phonon modes is very important, and must be taken into account in all electronic or optical investigations.

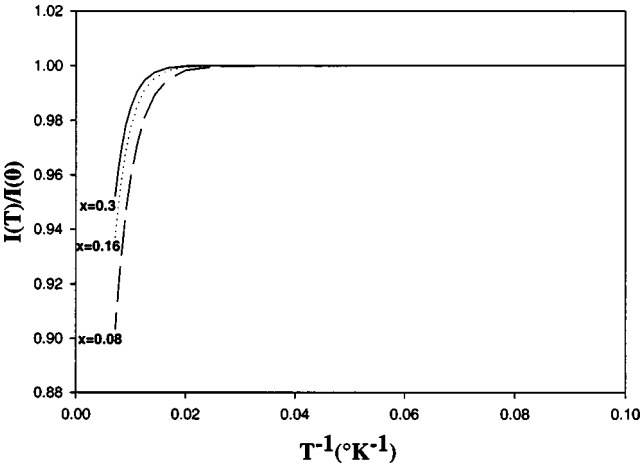

FIG. 6. Arrhenius plot of the integrated PL intensities ratio of CdTe QD of sizes $R=H=1a_{ex}^*$ embedded in $Cd_{1-x}Zn_xTe$ barrier material of Zn fraction $x=0.08$ (dashed line), 0.16 (dotted line), and 0.3 (solid line).

ACKNOWLEDGMENTS

This work has been supported by the Programs-in-Aide for Scientific Research (PASR) Physique 16 Oujda.

[1] Z. Xiao, J. Zhu, and F. He, Phys. Status Solidi B **191**, 401 (1995).
[2] F. J. Ribeiro, A. Latgé, M. Pacheco, and Z. Barticevic, J. Appl. Phys. **82**, 270 (1997).
[3] M. Mosko, D. Munzar, and P. Vagner, Phys. Rev. B **55**, 15416 (1997).
[4] M. Bayer, S. N. Walck, T. L. Reinecke, and A. Forchel, Phys. Rev. B **57**, 6584 (1998).
[5] R. Zheng and M. Matsuura, Phys. Rev. B **58**, 10769 (1998).
[6] P. Villamil and N. Porras-Montenegro, J. Phys.: Condens. Matter **10**, 10599 (1998).
[7] J. Zhu, S. Zhu, Z. Zahu, Y. Kawazoe, and T. Yao, J. Phys.: Condens. Matter **10**, L583 (1998).
[8] A. Montes, C. A. Duque, and N. Porras-Montenegro, J. Phys.: Condens. Matter **10**, 5351 (1998).
[9] H. Gotoh and H. Ando, Phys. Rev. B **96**, 1667 (1997).
[10] P. Villamil, N. Porras-Montenegro, and J. C. Granada, Phys. Rev. B **59**, 1605 (1999).
[11] A. Motes, C. A. Duque, and N. Porras-Montenegro, Phys. Status Solidi B **220**, 181 (2000).
[12] C. Garcia and I. D. Mikhailov, Phys. Status Solidi B **220**, 201 (2000).
[13] E. Reyes-Gomez, A. Matos-Abiague, M. De Dios-Leyva, and L. E. Oliveira, Phys. Status Solidi B **220**, 71 (2000).
[14] L. M. Hernandez-Ramirez and I. Hernandez-Calderon, Phys. Status Solidi B **220**, 205 (2000).
[15] A. V. Gopal, R. Kumar, and A. S. Vengulekar, J. Appl. Phys. **87**, 1858 (2000).
[16] J. T. Devreese, V. M. Fomin, V. N. Gladilin, and S. N. Klimin, Phys. Status Solidi B **224**, 401 (2001).
[17] R. Zheng, M. Matsuura, and T. Taguchi, Phys. Rev. B **61**, 9960 (2000).
[18] H. Han and H. N. Spector, Phys. Rev. B **62**, 13599 (2001).
[19] J. T. Devreese, *Polaron*, in Encyclopedia of Applied Physics, (VCH, Weinheim, 1996) Vol. 14, p. 383.
[20] V. V. Zaïtsev, V. S. Bagaev, and E. E. Onishchenko, Phys. Solid State **41**, 647 (1999).
[21] V. S. Bagaev, V. V. Zaïtsev, E. E. Onishchenko, and Yu. G. Sadofyev, J. Cryst. Growth **214/215**, 250 (2000).
[22] V. S. Bagaev, V. V. Zaïtsev, and E. E. Onishchenko, BRAS Phys. **64**, 260 (2000).
[23] H. P. Wagner, H. P. Tranits, R. Schuster, G. Bacher, and A. Forchel, Phys. Rev. B **63**, 155311 (2001).
[24] J. Zhao, S. V. Nair, and Y. Masumoto, Phys. Rev. B **63**, 033307 (2001).
[25] N. Kim, G. Ihm, H. S. Sim, and T. W. Kang, Phys. Rev. B **63**, 235317 (2001).
[26] G. Murillo and N. P. Montenegro, Phys. Status Solidi B **220**, 187 (2000).
[27] M. Bouhassoune, R. Charrour, M. Fliyou, D. Bria, and A. Nougaoui, J. Appl. Phys. **91**, 232 (2002).
[28] N. Dai, F. Brown, R. E. Doezema, S. J. Chung, and M. B. Santos, Phys. Rev. B **63**, 115321 (2001).
[29] R. Hellman, M. Koch, J. Feldmann, S. T. Cundiff, E. O. Göbel, D. R. Yakovlev, A. Waag, and G. Landwehr, Phys. Rev. B **48**, 2847 (1993).
[30] M. O'Neill, M. Oestreich, W. W. Rühle, and D. E. Ashenford, Phys. Rev. B **48**, 8980 (1993).
[31] H. E. Porteanu, E. Lifshitz, M. Pflughoefft, A. Eychmüller, and H. Weller, Phys. Status Solidi B **226**, 219 (2001).
[32] Y. Masumoto, M. Ikezawa, B. R. Hyun, K. Takemoto, and M. Furuya, Phys. Status Solidi B **224**, 613 (2001).
[33] S. V. Branis, G. Li, and K. K. Bajaj, Phys. Rev. B **47**, 1316 (1993).
[34] Y. Kayanuma, Phys. Rev. B **44**, 13085 (1991).
[35] T. D. Lee, F. Low, and D. Pines, Phys. Rev. **90**, 297 (1953).
[36] R. Charrour, M. Bouhassoune, M. Fliyou, D. Bria, and A. Nougaoui, J. Phys.: Condens. Matter **12**, 4817 (2000).
[37] S. Le Goff and B. Stébé, Phys. Rev. B **47**, 1383 (1993).
[38] D. G. Ctchekline, G. D. Gilliland, Z. C. Feng, S. J. Chua, D. J. Wolford, S. E. Ralph, M. J. Schurman, and I. Ferguson, MRS Internet J. Nitride Semicond. Res. **4S1**, G 6.47 (1999).